

Phonon production in weakly photoexcited semiconductors: Quasidiffusion in Ge, GaAs, and Si

M. E. Msall

Department of Physics, Bowdoin College, Brunswick, Maine 04011

J. P. Wolfe

Materials Research Laboratory and Department of Physics, University of Illinois at Urbana-Champaign, Urbana, Illinois 61801

(Received 23 August 1996; revised manuscript received 28 March 1997)

Nonequilibrium phonon propagation is observed in Ge, Si, and GaAs at $T=2.2$ K when these materials are weakly photoexcited with a pulsed Ar^+ laser (typically a defocused 10 ns, nanojoule pulse). The overall shapes of the experimental heat pulses agree well with computer simulations incorporating anisotropic phonon propagation (phonon focusing effects), isotope scattering, and anharmonic decay. Quantitative comparisons between the experimental and theoretical decay rates lead us to conclude that (1) although surface reflections near the excitation point play a key role in determining the character of the detected phonon energy, reflections from the sample sidewalls appear to have a smaller effect at times of interest in the experiment; (2) the agreement between the experimental data and our theoretical models of quasidiffusion is better for silicon than for germanium or gallium arsenide. These moderate discrepancies (factors of about 2 in decay rates) are attributed to uncertainties in the elastic-scattering rate and/or anharmonic decay rate. Overall, the basic model of quasidiffusive phonon propagation is quite successful in predicting the principle features of nonequilibrium phonon propagation following direct photoexcitation of a semiconductor. [S0163-1829(97)01636-6]

I. INTRODUCTION

The scattering processes of acoustic phonons in nonmetallic solids can be effectively studied by observing the transmission of heat pulses across a sample at low temperatures. To gain quantitative information, however, one must have good control over the production and detection of nonequilibrium phonons. Heat-pulse experiments generally utilize one of two modes of excitation: (a) direct photoexcitation of the crystal, and (b) excitation of a metal film deposited on the surface of the crystal. Phonon imaging experiments by Shields and Wolfe¹ in Si indicated that the transmitted phonon signals in a direct photoexcitation experiment were very similar to those of phonons generated by metal-film heating. This was a surprising result in view of the large difference between phonon-carrier interactions in metals and semiconductors at low temperatures. In particular, the relaxation rate of high-frequency nonequilibrium phonons in metals is expected to be much faster than that in semiconductors. Later experiments by Shields *et al.*² found that the similarities between the results for the two excitation conditions were an artifact of the surface conditions: the presence of liquid helium at the excitation surface greatly altered the evolution of the phonon system. Thus, the ability to effectively isolate the excitation surface from the helium bath has proven critical to the study of the intrinsic relaxation of the phonon-carrier system.

Making use of this discovery, we have found that there are different regimes of phonon production in photoexcited semiconductors accessed by changing the excitation power. Indeed, the "excitation density," or absorbed laser power per area, proves to be the effective control parameter in such experiments. The dependence of phonon scattering on excitation density is associated with the formation of various

excitonic phases produced by the photoexcited carriers. In this paper, we will limit ourselves to the regime of low excitation density, where condensed electron-hole phases (electron-hole liquid) do not form. In this regime the excited carriers shed much of their excess energy by emitting optical phonons rather than through interactions with other carriers. These optical phonons do not travel far in the crystal before anharmonic processes split them into lower-frequency acoustic phonons. As the phonons diffuse into the bulk of the crystal, they continue to cascade down to lower frequencies. The combination of diffusion and anharmonic decay is called "quasidiffusion"³ and results in an extended heat pulse dominated by scattered phonons.

In this paper, we compare the acoustic-phonon propagation in the semiconductors Si, Ge, and GaAs following direct photoexcitation. The baseline for our model of phonon scattering in semiconductors is silicon, where elastic and inelastic scattering processes are reasonably well characterized. Isolated-surface excitation of silicon led to the first observations and quantitative characterizations of quasidiffusion in a pure semiconductor.² Theoretical models of quasidiffusion were successfully developed for these silicon experiments by Tamura⁴ and Esipov.⁵ In this work, we have attempted to capitalize on the success of these models in describing quasidiffusion in Ge and GaAs, as well as in Si. In doing so, we set useful limits on the range of assumptions under which the analytic and computer models can be considered relevant to the experimental conditions.

The experimental observations of quasidiffusion require relatively weak levels of photoexcitation. The shape of the phonon pulse changes radically at higher excitation levels where dense electron-hole plasmas form. At high powers, the heat pulses still exhibit long decay "tails," but the relative abundance of ballistic (i.e., unscattered), low-frequency

phonons increases dramatically. In effect, at high powers, low-frequency phonons are being produced more efficiently than can be accounted for by the phonon cascade. In fact, the amount of energy in these ballistic phonons is still small compared to the total energy in the phonon system, but the ballistic signals are readily observable because phonon focusing concentrates the ballistic energy spatially. Indeed, a small amount of energy bypassing the normal optical-phonon cascade into the ballistic range causes a notable change in the shape of the phonon time traces. Consequently, the heat-pulse signals are quite sensitive to the phonon down-conversion processes near the excitation point. The ballistic phonons produced under high excitation conditions cannot be accounted for in the quasidiffusive model and will be discussed in a later paper.

II. EXPERIMENTAL DETAIL

The experiments described in this paper use the heat-pulse and phonon-imaging techniques described in an earlier work.^{1,2} The samples were as follows: (1) A $2.6 \times 3 \times 1.35$ mm³ [100]-oriented GaAs crystal. This sample, provided by W. E. Bron of the University of California at Irvine, was meltgrown by Wacker Chemitronics in a BN crucible. It is ‘‘chromium free’’ with a resistivity of $\rho = 10^6$ Ω cm. (2) An $8 \times 9.1 \times 3$ mm³ [100]-oriented ultrapure dislocation-free Ge crystal. This crystal (Boule 146) was grown by E. E. Haller at Lawrence Berkeley Laboratory. (3) Two Si samples were grown by Siemens, one with dimensions $6.6 \times 7.0 \times 5.4$ mm³ the other $8.9 \times 8.7 \times 2.75$ mm³. Both are characterized by $N_A - N_D = 10^{12}$ cm⁻³.

For all crystals, the excitation and detection faces are {100} planes. The samples were mechanically polished with an alumina suspension and polished and/or etched with Syton to remove subsurface damage. The detectors are 10×5 μm^2 granular aluminum bolometers directly evaporated on the (100) faces, with superconducting transitions just below 2 K. Direct photoexcitation of the detectors with a 10-ns pulse from the Ar⁺ laser typically produced a pulse with 70-ns full width at half maximum. To obtain the weak photoexcitation conditions necessary to observe quasidiffusion in Si and Ge, the laser spot size was defocused to 50–100 μm . For GaAs, the lifetime of the photoexcited carriers is much shorter than in Si and Ge; therefore a sharper focus (10–20 μm) could be used without producing high densities of excited carriers.

All experiments are performed with direct photoexcitation of the crystal surface, using a sample holder which isolates the excitation surface from the He bath. The detector surface and the four sidewalls are always in contact with the liquid He at 1.7 K.

III. ANALYTIC THEORY OF QUASIDIFFUSION

In the simple quasidiffusive model,³ phonons are viewed as a succession of diffusively propagating ‘‘generations’’ which evolve into ballistic phonons. On average, each phonon generation has one-half the frequency of its parent generation. In a sample of thickness d , ‘‘ballistic phonons’’ (those with $V\tau_i > d$, where V is the phonon velocity) have frequencies, $\nu < \nu_{\text{cutoff}}$ such that

$$\nu_{\text{cutoff}} = \left(\frac{V}{Ad} \right)^{1/4}, \quad \nu_{\text{parent}} \approx 2\nu_{\text{cutoff}}, \quad (1)$$

where the isotope scattering rate,

$$\tau_i^{-1} = A\nu^4, \quad (2)$$

is considered to be independent of phonon mode. Since the lifetime of each generation increases rapidly it is reasonable in a first approximation to ignore the effect of comparatively short-lived higher generations and assume that all the phonons are produced by the anharmonic decay of a single parent frequency, ν_{parent} . Thus, the rate of anharmonic decay,

$$\tau_a^{-1} = B\nu^5, \quad (3)$$

sets the time scale for a phonon generation. Dispersion of the phonon modes severely constrains the allowed channels of anharmonic decay, so that the value of the anharmonic decay constant B is highly mode dependent. In all of the following calculations, we substitute a mode-averaged decay constant B_{avg} . In calculating this average, contributions from different phonon modes are weighted by the density of phonon states.

In the simple quasidiffusive model, the ‘‘source region’’ for the ballistic phonons is a hemisphere with a radius equal to the diffusion length of the parent generation, i.e., the average distance diffused before anharmonic decay,

$$I_{\text{parent}} = \left(\frac{V^2}{3} \tau_i(\nu_{\text{parent}}) \tau_a(\nu_{\text{parent}}) \right)^{1/2} = \left(\frac{V^2}{AB2^9} \left(\frac{dA}{V} \right)^{9/4} \right)^{1/2} \\ = \frac{d^{9/8} A^{5/8}}{2^{9/2} \sqrt{B} V^{1/8}}. \quad (4)$$

The ballistic-phonon source size is expected to scale with the sample thickness to the $\frac{9}{8}$ power. For a 1.35-mm-thick GaAs sample, this model predicts a source size of about 400 μm .

The phonon image of GaAs shown in Fig. 1 vividly demonstrates that this is not the case. Indeed, the phonon source size predicted by this model is larger than the slow transverse-box structure dominating the image. The experimental image contains many clearly resolved structures which are much smaller than 400 μm . Specifically, the measured caustic width in this experiment, corresponding to a 10–90 % rise in phonon signal, requires only about an 18- μm displacement of the laser beam. This distance is assumed to be the size of the ‘‘phonon source’’ region, that is, the region in which ballistic phonons are produced. Of course, the experimental image only samples the phonons detected in a specified time interval, in this case within 250 ns of the first phonon arrivals at the detector. The distance diffused by the parent generation in the first 100 ns of the phonon evolution is more nearly 100 μm , which is still much greater than the experimentally measured phonon source size.

The reason for this discrepancy, in part, is that the theory does not take into account the distribution of phonons produced in a single down-conversion event. Because of the distribution of possible decay paths, ballistic phonons can be produced in a single decay of a high-frequency phonon. Such events, yielding one very-low-frequency phonon and one

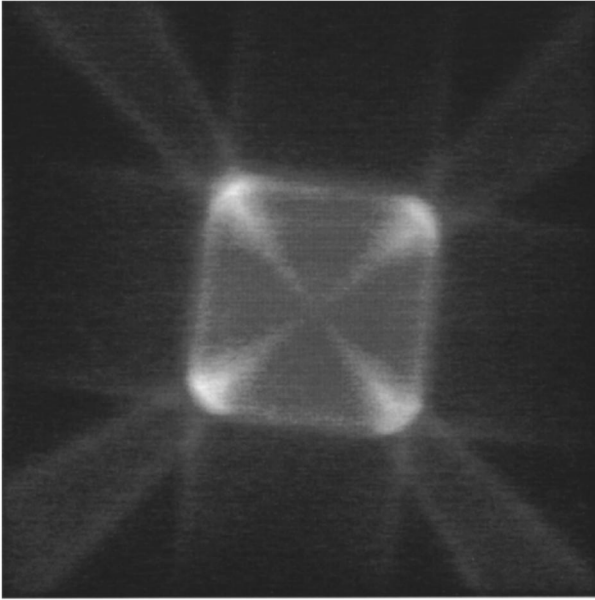


FIG. 1. Experimental phonon image of [100] GaAs. The 1.35-mm-thick crystal is directly photoexcited with a 10-ns pulse from a 10-mW Ar⁺ laser. The laser spot is focused on the sample surface for an excitation density of about 50 W/mm². The data are collected over a fixed time interval ($t_b < t < 1.5t_b$). The distance scanned by the laser over the entire image is about 500 μm . Unlike other published images of photoexcited semiconductors, this image does not have liquid helium at the excitation surface, a point which plays a large role in the properties: The excitation surface is in vacuum.

higher-frequency phonon are less likely than the production of two phonons of roughly equal frequency, but still possible. The very-low-frequency phonons produced in this manner would be the source of ballistic phonons produced near the excitation point. This early ballistic phonon production combined with the strong effects of phonon focusing would make the caustic structures in the phonon images appear sharp, affecting the experimental estimate of the phonon source size. For this reason, it is more reasonable to apply the simple quasidiffusive theory only to the late-time signal, or to consider computer models that take into account the partition of energy in anharmonic decay events.

IV. COMPUTER MODELS OF QUASIDIFFUSION

The first computer simulations of quasidiffusion conducted by Maris assumed complete isotropy in the phonon propagation and scattering.⁶ The results of a more detailed simulation which includes anisotropies in propagation are shown in Fig. 2(a). This simulation includes the effects of noncollinearity of wave-vector and group velocity directions and the resulting phonon-focusing effect but assumes that the anharmonic decay process is collinear. In particular, anharmonic decay is assumed to leave the phonon mode and wave vector unchanged but split the original phonon according to the probability distribution

$$P(\omega_i \rightarrow \omega_f) \propto \omega_f^2 (\omega_i - \omega_f)^2, \quad (5)$$

where ω_i is the initial phonon frequency, and the final phonon frequencies are ω_f and $\omega_i - \omega_f$.

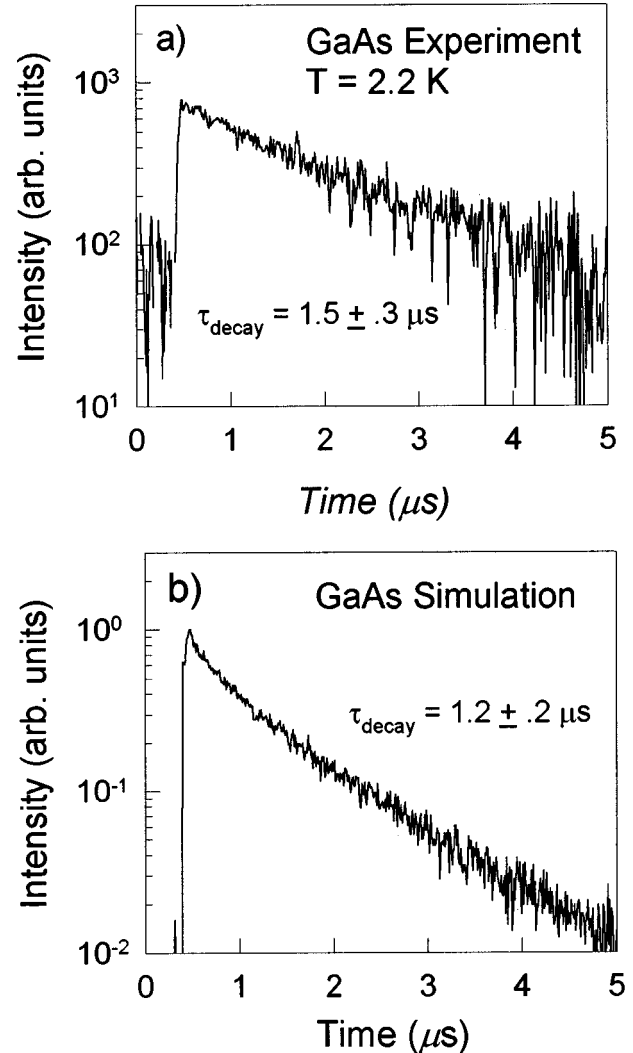


FIG. 2. (a) Intensity of the phonon signal vs time along the [100] propagation direction for weakly photoexcited ($P/A \approx 10 \text{ W/mm}^2$) GaAs of 1.35 mm thickness, with a vacuum at the excitation surface. The characteristic decay time is $1.5 \pm 0.3 \mu\text{s}$. The laser spot is focused to a 10- μm radius. (b) Monte Carlo simulation of quasidiffusion in a 1.35-mm-thick GaAs sample. This simulation begins with 2-THz phonons in an infinite slab. The isotope scattering and anharmonic decay constants are $A = 7.38 \times 10^{-42} \text{ s}^3$ and $B_{\text{Avg}} = 1.13 \times 10^{-55} \text{ s}^4$. The signal decay is exponential with a characteristic decay time of $1.2 \pm 0.2 \mu\text{s}$ in agreement with the prediction of the bottleneck model for slab geometry.

During the computed isotope scattering processes, the phonon frequency is unchanged but the wave-vector direction is randomized and a new mode is chosen in accordance with the density-of-states factors. These simulations include anisotropy when determining phonon trajectories, but do not take anisotropy into account when assigning anharmonic decay or isotope scattering results because a large increase in computational complexity would ensue. Although the elastic scattering anisotropy is expected to play a large role in the propagation of once or twice scattered phonons⁷ the effect is greatly reduced after multiple scattering events, and should therefore be small for quasidiffusive propagation.

The shape of the simulated heat pulse can be characterized by the falloff in the phonon intensity arriving at the

TABLE I. Parental parameters. Phonon parameters for the crystals under consideration: d is the crystal thickness; V is measured transverse velocity along the 100 direction; A is the calculated isotope-scattering constant [S. Tamura, Phys. Rev. B **27**, 858 (1983)]; B_{Avg} is the calculated mode-averaged anharmonic-decay constant; ν_{parent} and l_{parent} are defined by Eqs. (1) and (4).

System	d (mm)	$V_s[100]$ TA (cm/s)	A (s^3)	B_{Avg} (s^4) ⁴	ν_{parent}	l_{parent} (mm)
Si	5.5	5.86×10^5	2.43×10^{-42}	1.2×10^{-56}	1.6 THz	2.3
Ge	3	3.58×10^5	3.67×10^{-41}	1.61×10^{-55}	850 GHz	1.7
GaAs	1.35	3.35×10^5	7.38×10^{-42}	1.13×10^{-55}	1.5 THz	0.36

detector at late times. It turns out that, if the data are plotted on a semilogarithmic scale, this falloff can usually be fit to a single exponential at late times. Consequently, a characteristic decay time can be defined. The value of this characteristic decay time for Si from a model similar to the one above agrees very well with the fits to experimental data.⁸ The experimental observation of quasidiffusion required elimination of the phonon losses into the helium bath at the excitation surface and very weak photoexcitation with a defocused laser.

In GaAs, it is possible to see quasidiffusive time traces even with low power *focused* excitation as shown in Fig. 2(a). The experimental heat pulse displays a sharp onset at the ballistic arrival time of transverse phonons and a long tail of scattered phonons, qualitatively similar to the form predicted for quasidiffusing phonons. If the signal at late times is fit to an exponential, the experimentally measured decay time is $\tau_d = 1.5 \pm 0.3 \mu\text{s}$.

The computer model reproduces the shape of the time trace near the ballistic time as well as the monotonically decaying tail. If the late time signal of the simulated time-trace is fit to an exponential, however, the relaxation time is $1.15 \mu\text{s}$, which is just outside the error bars on the experimental measurement. A larger value of the anharmonic decay constant would increase the predicted relaxation time and improve the agreement between the simulation and the experiment.

The extreme sensitivity of the quasidiffusive simulations to the assumed intrinsic scattering rates suggests that this measurement might be used as a gauge of calculated values (see below). Presently, the third-order elastic constants in GaAs have not been measured at low temperatures, and the room-temperature values measured by two independent groups⁹ vary enough to cause a 40% change in the calculated decay rates.¹⁰

In addition to the uncertainty in the anharmonic decay rate, the total rate of elastic scattering in GaAs is also uncertain. Measurement of the phonon scattering in this GaAs sample by Ramsbey, Tamura, and Wolfe¹¹ has shown high rates of transverse phonon scattering, consistent with an elastic-scattering constant which is four times larger than the predicted isotope scattering constant for GaAs. The measurement of longitudinal-phonon scattering is consistent with the predicted value for isotope scattering. The authors suggest that the difference in scattering rates for transverse phonons is due to an extrinsic defect in the GaAs.

V. LOSSES AT THE SAMPLE BOUNDARIES

One interesting characteristic of both the experimental and simulated time traces is that they can be fit to a single

exponential at late times. The simplest explanation for this decay is that it is related to the production time for ballistic phonons. And indeed, the anharmonic decay time for a phonon with frequency equal to ν_{parent} in our GaAs sample (Table I) is comparable to the decay time of the experimental pulse.

However, there is nothing in the simple quasidiffusive model which would lead us to suspect such an exponential form. A more detailed analytic model of quasidiffusion, articulated by Esipov,⁵ does explicitly predict such a form. Although there is no single diffusion constant describing quasidiffusive phonon propagation, quasidiffusion can still be modeled using a modified diffusion equation. According to Esipov's analysis, the solution of this modified diffusion equation may indeed be dominated by a single-phonon frequency at late times, leading to an exponential falloff in the phonon signal. The dominant, "bottleneck," frequency is determined by a balance between the production rate of low-frequency (ballistic) phonons and the diffusion of higher frequencies.

The predicted bottleneck frequency for a slab with face dimensions $2L_x$ and $2L_y$ and sample thickness L_z is

$$\nu_{\text{BN}} = \left(\frac{4V^2\pi^2}{15ABL^2} \right)^{1/9} \quad \text{with} \quad \frac{1}{L^2} = \frac{1}{4} \left(\frac{1}{L_x^2} + \frac{1}{L_y^2} + \frac{1}{L_z^2} \right). \quad (6)$$

This results in a predicted relaxation rate:

$$\tau_0^{-1} = 2.25B\nu_{\text{BN}}^5 = 3.85 \left(\frac{V^{10}B^4}{L^{10}A^5} \right)^{1/9}. \quad (7)$$

Values of the bottleneck frequency for our Si, GaAs, and Ge samples are listed in Table II. When these values are compared to ν_{parent} from the generations model (See Table I) we find that $\nu_{\text{parent}} \approx \nu_{\text{BN}}$. Because of the strong frequency dependence of the relaxation rates and the geometry-dependent prefactor, the value of the decay rate predicted by the bottleneck model is quite different from the simple anharmonic decay rates of the parent phonon generation. At late times the model predicts that the phonon signal intensity will fall off like the production rate of ballistic phonons, with a decay rate that depends upon the sample geometry.

The relaxation rates predicted by Eq. (7) (shown in Table II) are expected to be faster than those observed experimentally because of the way in which the analytic model treats the sample sidewalls. The boundary condition in the computer model is that the sidewalls are perfect phonon absorbers. This is not a realistic description of the sample-liquid-

TABLE II. Bottleneck frequencies and decay times (slab geometry). A comparison of calculated signal decay parameters [Eqs. (6) and (7)] and experimental decay times for our samples. The experimental decay time is determined by fitting the phonon signal to a single exponential at late times.

Material	Sample dimensions (L_x, L_y, L_z) (mm)	ν_{BN} (THz)	Bottleneck model τ_0 (μs)	Experimental decay time (μs)
Si	3.3,3.5,5.4	1.76	2.2	3.4 ± 0.3
Si	4.5,4.4,2.75	1.78	2.07	1.5 ± 0.2
Ge	4.0,4.6,3.0	0.88	5.4	2.7 ± 0.2
GaAs	2.6,3.0,1.35	1.3	1.2	1.5 ± 0.3

helium boundary, which is typically assumed to have 50% losses due to the Kapitza anomaly.

Figure 3(a) shows a time trace along the [100] direction of a 5.5 mm-thick Si crystal following very weak photoexcita-

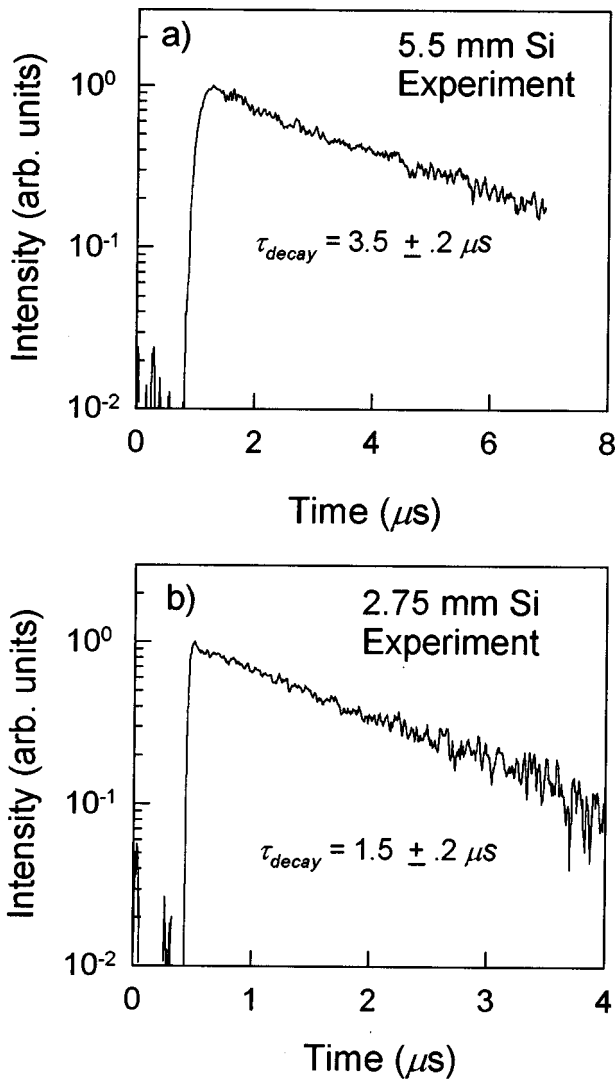


FIG. 3. Comparison of quasidiffusive time traces for two sample thicknesses. The excitation density in both cases is about 5 W/mm^2 . (a) The 2.75-mm-thick Si sample has a measured relaxation time of $1.5 \pm 0.2 \mu\text{s}$. The ballistic arrival time along this [100] direction is 480 ns. (b) The 5.5-mm-thick Si sample has a measured relaxation time of $3.4 \pm 0.2 \mu\text{s}$. The ballistic arrival time along this [100] axis is 950 ns. Note that the horizontal axes in the two figures differ by a factor of 2.

tion (about 50 nJ/mm^2 for a 10-ns pulse). In this experiment, the exponential decay constant ($3.4 \mu\text{s}$) is slower than the predicted relaxation time from the bottleneck model ($2.2 \mu\text{s}$, Table II). It is, however, in very good agreement with previously published simulations⁴ of quasidiffusion in Si ($3.6 \times t_b = 3.4 \mu\text{s}$), which assumed that the sample sidewalls were far enough away so that any sidewall losses were negligible.

A comparison of samples of different thicknesses supports the idea that sidewall losses do not have a large effect on the experimentally observed decay rates. The decay of the phonon signal at late times depends upon the sample dimensions through the parameter L^2 [defined in Eq. (6)]. For our two Si samples, $L = 2.2 \text{ mm}$ for the 5.4-mm-thick sample and $L = 2.07 \text{ mm}$ for the 2.7-mm-thick sample. The values of L for these samples are almost equal in spite of the factor of 2 difference in sample thickness because of the difference in face dimensions. In essence, L is a measure of the distance from the excitation point to the nearest loss point. In the 2.75 mm sample, the nearest loss point is the detector which is directly opposite the excitation surface; in the 5.5-mm sample, the nearest loss point is on the sample sidewall. The ratio of the two L values is about 1.1, so the predicted relaxation rates [Eq. (7)] which go as $L^{10/9}$, are nearly equal in the two samples.

The two experimental time traces shown in Fig. 3 emphatically disagree with this prediction. The relaxation of the signal in the thinner sample is a factor of 2.3 faster than in the thicker sample. This suggests that the pertinent length scale in the problem is not L but the sample thickness. In other words, phonon losses at the sample sidewalls do not appear to have a large effect on the quasidiffusive decay time. If we set L_x and L_y equal to infinity in Eq. (7), the expected change in relaxation rates between the two samples is a factor of 2.2, in reasonable agreement with the experimental measurement.

It is initially puzzling that the losses at the sample sidewalls do not have a larger effect on the phonon time traces when the losses into the helium are expected to be great. It is less surprising when one considers the distance from the excitation point to the sidewalls. In the 5.4-mm-thick sample, the detector is positioned so that the [100] point on the excitation surface is about 3 mm from any sidewall. A phonon traveling ballistically to the sidewall and back towards the detector will add at least a microsecond to its time of flight ($v \approx 5 \times 10^5 \text{ cm/s}$). Because of this, sidewall scattering will not affect the shape of the timetrace until late times.

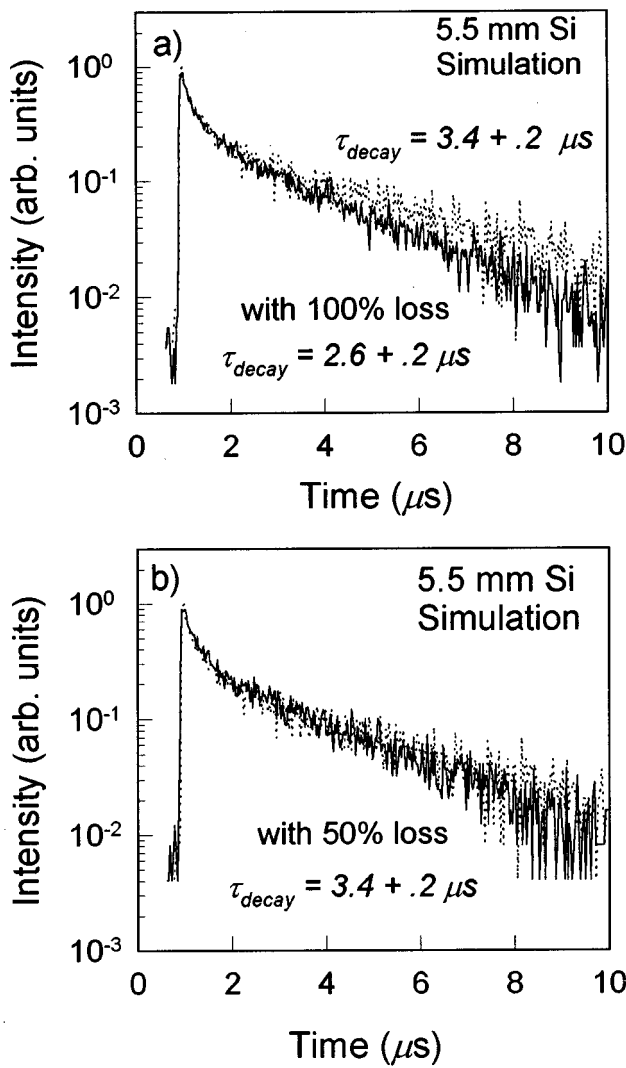


FIG. 4. (a) At early times ($< 2 \mu\text{s}$) a Monte Carlo simulation of phonon propagation along the $[100]$ direction including phonon losses from the sample sidewalls (solid line) is not very different from one in which the planar dimensions of the slab are infinite (dotted line). The decrease in signal at late times, however, is very different. The expected relaxation time for the $6.6 \times 7 \times 5.4 \text{ mm}^3$ Si sample (the finite slab) is 1.3 times greater than that of the infinite slab, which agrees well with the ratio of relaxation times from the Monte Carlo simulations ($3.4/2.6 = 1.3$). (b) The resemblance between simulated time traces for a finite and an infinite slab increases if 50% of the phonons incident on the sample sidewall in the finite slab are reflected back into the sample. In this case, the finite slab (solid line) is indistinguishable from the infinite slab (dotted line) for times less than $6 \mu\text{s}$. At late times, the signal relaxation in the finite slab is faster.

A Monte Carlo simulation using the geometry of the 5.5-mm-thick sample, in which phonons which pass the sidewall are discarded (simulating a perfectly lossy boundary) is shown as a solid line in Fig. 4(a) along with a simulation in which the slab is infinite (dotted line). At times less than $3 \mu\text{s}$, the two simulations are indistinguishable, but the relaxation time at late times is much shorter for the sample with a lossy boundary. If the boundary is not perfectly absorbing,

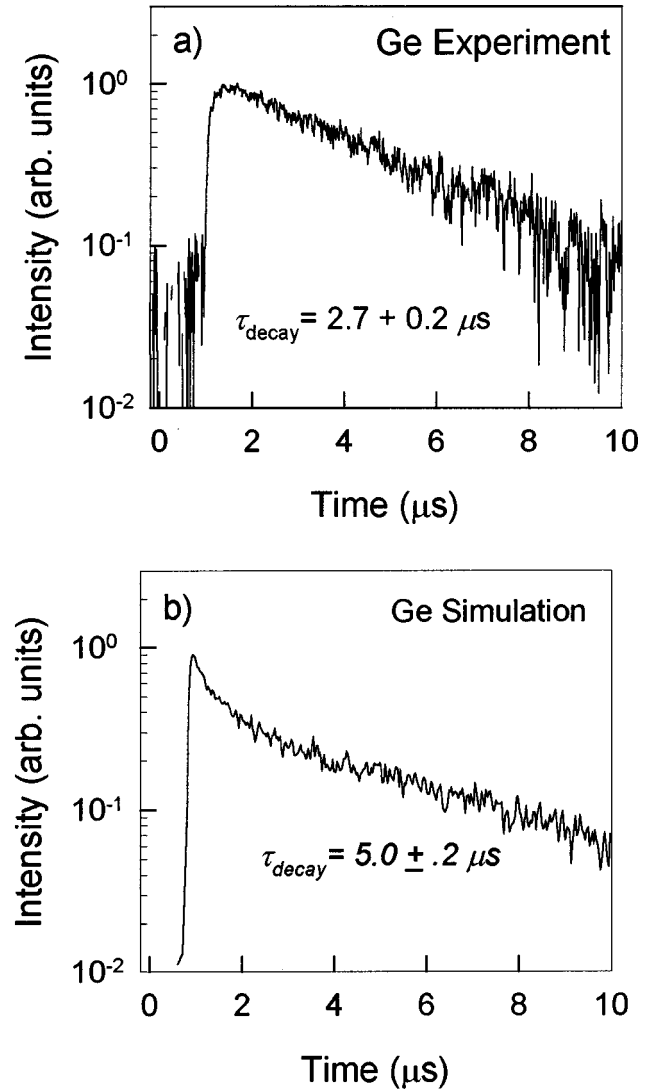


FIG. 5. (a) Intensity of the phonon signal vs time along the $[100]$ propagation direction for weakly photoexcited ($P/A \approx 5 \text{ W/mm}^2$) Ge of 3 mm thickness. The characteristic decay time is $2.7 \pm 0.2 \mu\text{s}$. The time between successive laser pulses is $80 \mu\text{s}$. Observations of quasidiffusion in Ge are sensitive to the pulse repetition time. If the laser pulse separation is not greater than the $40 \mu\text{s}$ carrier lifetime in electron-hole liquid, a shorter decay time is observed. (b) Monte Carlo simulation of quasidiffusion in a 3-mm-thick Ge sample. This simulation begins with 2-THz phonons in an infinite slab. The isotope and anharmonic decay scattering constants $A = 2.43 \times 10^{-42} \text{ s}^3$ and $B_{\text{avg}} = 1.61 \times 10^{-55} \text{ s}^4$. At late times the signal decay is exponential with a characteristic decay time of $5.0 \pm 0.2 \mu\text{s}$, which is slightly less than the $5.4 \mu\text{s}$ predicted by the bottleneck model for slab geometry.

but reflects 50% of the incident phonons back into the sample, the effect on the phonon timetraces is even smaller. A Monte Carlo simulation of a sample with 50% boundary loss, shown in Fig. 4(b), is indistinguishable from the infinite slab for times less than $6 \mu\text{s}$. Thus, if one wishes to observe the effects of sample geometry on the relaxation time, one must carefully examine the signal at very late times. Unfortunately, at these late times, the experimental phonon signal is usually small and it is difficult to fit to an exponential.

Thus, our measurement of the decay rate of Si is consistent with models that ignore phonon losses at the sample sidewalls.

VI. A COMPREHENSIVE MODEL?

The fact that the experiment and theory for Si show overall consistency is very encouraging, but the data for Ge and GaAs do not follow the same trend. For GaAs, the prediction of the characteristic decay time from the bottleneck model for slab geometry is barely within the experimental uncertainty. However, if we assume, as we did for Si, that the sidewall losses are negligible, then the agreement between experiment and theory is no longer so good. Remembering our earlier comments about the uncertainty of the calculated scattering rates for GaAs, we may attribute this discrepancy to the assumed value of these constants. In the bottleneck model, the characteristic decay time goes as $A^{5/9}/B^{4/9}$, where A and B are the isotope scattering anharmonic decay constants, respectively. The variation in published values of A ($7.38 \times 10^{-42} \text{ s}^3$ or $2.9 \times 10^{-41} \text{ s}^3$) and B ($7.72 \times 10^{-55} \text{ s}^4$ or four times this value) yield values for the calculated relaxation time of the phonon signal which range from 1.2 to 4.6 μs . Since our experimental measurement falls within this range, we are unable to make any strong conclusions about the calculated values of the scattering constants.

For Ge, the disagreement between the analytic and computer models and the experimental results is especially striking. The predicted decay time of around 5 μs is much larger than the experimentally observed value of 2.7 μs shown in Fig. 5. Our computer simulations have shown that there is little effect on the predicted decay time if the initial phonon distribution is assumed to be broadly spread as long as the average phonon frequency in the distribution is greater than the bottleneck frequency for the sample. This condition is met by choosing an initial phonon frequency of 2 THz for our Ge simulation.

One of the notable differences between phonons in Ge and those in Si or GaAs is the very low frequency of the zone-boundary phonon in Ge. In order to assume the mode-averaged anharmonic decay rate in the simulation the phonons must undergo mode-converting isotope scattering much more frequently than anharmonic decay. In Si and GaAs this was a safe assumption for phonon frequencies as high as 4 THz. In Ge, however, this cannot be assumed for phonon frequencies greater than 2 THz. Above this frequency, which is that of the lowest zone-boundary TA phonon, the isotope scattering and anharmonic decay rates deviate from their low-frequency form. A calculation by Okubo and Tamura¹² of the effect of lattice dispersion upon the decay rates of LA phonons of 2-THz phonons shows that the anharmonic decay rates of these phonons do not differ from those extrapolated from the low-frequency rates. The isotope scattering rate at 2 THz is increased from the low-frequency rate by a factor of 10, but such a correction would increase rather than decrease the characteristic decay time of the simulation. If the pertinent frequencies were more like 4 THz, the corrections to both decay rates would work to decrease the characteristic decay time. However, this frequency is so much greater than the bottleneck frequency, it is unrea-

sonable to assume that these frequencies greatly influence the quasidiffusive process.

Another possible reason for the shorter decay time in the experimental time trace is that contributions from the decay of TA phonons significantly alter the anharmonic decay constant. To date, there has been no calculation of the TA decay in Ge, but if we assume that the TA decay occurs in the same ratio to the L decay as predicted by Berke, Mayer, and Wehner¹³ for Si (about $\frac{1}{3}$ the rate), the resultant mode-averaged decay rate is a factor of 2.7 larger. This factor is enough to bring the theoretical prediction for τ_{decay} in line with the experiment. However, inclusion of anharmonic decay within the T branches in the Si simulation would tend to worsen the agreement between theory and experiment.

VII. CONCLUSIONS

The theoretical models of quasidiffusion are sensitive to the assumed anharmonic decay rates and elastic-scattering rates, implying that heat-pulse measurements in this scattering regime provide experimental input on these parameters. In Si, the agreement between the experimental data and the theoretical models is good when the effects of TA phonon decay and the sample sidewalls are neglected. Our computer simulations indicate that the effect of the sample sidewalls is small at times of interest in the experiment.

In GaAs there is also reasonable agreement between the theoretical predictions and the experimental data, but the theoretical predictions have a high degree of uncertainty because of the lack of certainty in the value of the low-temperature third-order elastic constants. In Ge, the quantitative predictions of the quasidiffusive models using currently calculated decay rates differ from the experimental data by a factor of 2. This may indicate that better calculations of the anharmonic decay rate are needed. The relative importance of the TA phonon decay in the three systems is in question. We find good agreement between theory and experiment in Si if we neglect this decay channel, but these results are not definitive. In all cases we have ignored any possible effects of phonon downconversion by surface defects.

We conclude that, in general, the model of quasidiffusive phonon propagation (diffusion plus decay) incorporating phonon focusing effects is a useful approach to understanding the propagation of nonequilibrium phonons following direct photoexcitation of a semiconductor. At the present stage of sophistication, the models yield decay rates within a factor of 2 of the experimental rates. This agreement is expected to improve with a better understanding of surface scattering and decay processes.

ACKNOWLEDGMENTS

This work has been supported by the National Science Foundation (Materials Research Laboratory Grant No. DMR 89-20538), the GANN Fellowship program, and Bowdoin College. We also wish to acknowledge many helpful discussions with Sergei Esipov and Shin Tamura.

- ¹J. A. Shields and J. P. Wolfe, *Z. Phys. B* **75**, 11 (1989).
- ²J. A. Shields, M. E. Msall, M. S. Carroll, and J. P. Wolfe, *Phys. Rev. B* **47**, 12 510 (1993).
- ³D. V. Kazakovtsev and I. B. Levinson, *Phys. Status Solidi B* **96**, 117 (1979).
- ⁴S. Tamura, *Phys. Rev. B* **48**, 13 502 (1993).
- ⁵S. E. Esipov, *Phys. Rev. B* **49**, 716 (1994).
- ⁶H. J. Maris, *Phys. Rev. B* **41**, 9736 (1990).
- ⁷M. T. Ramsbey, J. P. Wolfe, and S. Tamura, *Z. Phys. B* **73**, 167 (1988).
- ⁹M. E. Msall, S. Tamura, S. E. Esipov, and J. P. Wolfe, *Phys. Rev. Lett.* **70**, 3463 (1993).
- ¹⁰H. J. McSkinnon *et al.*, *J. Appl. Phys.* **38**, 2610 (1967).
- ¹¹Shin Tamura (private communication).
- ¹²M. T. Ramsbey, S. Tamura, and J. P. Wolfe, *Phys. Rev. B* **46**, 1358 (1992).
- ¹³K. Okubo and S. Tamura, *Phys. Rev. B* **28**, 4847 (1983).
- ¹⁴A. Berke, A. P. Mayer, and R. K. Wehner, *J. Phys. C* **21**, 2305 (1988).